

OMNI-DIRECTIONAL L-BAND ANTENNA FOR MOBILE COMMUNICATIONS

DR. C. S. KIM, N. MOLDOVAN, and J. KIJESKY
PRODELIN CORPORATION
1700 NORTHEAST CABLE DRIVE
P. O. BOX 368
CONOVER, NORTH CAROLINA 28613
UNITED STATES

ABSTRACT

This paper discusses the principle and design of our L-band omni-directional mobile communication antenna. The antenna is a circular waveguide aperture with hybrid circuits attached for higher order mode excitation. It produces circular polarized and symmetric two split beams in elevation. The circular waveguide is fed by eight probes with a 90 degree phase shift between their inputs. Radiation pattern characteristics are controlled by adjusting the aperture diameter and mode excitation. This antenna satisfies gain requirements as well as withstanding the harsh environment.

INTRODUCTION

This paper describes the development of a circular polarized, high gain, L-band transmit antenna for mobile communications. The antenna is a circular waveguide with an integrated stripline feed circuit to produce circular polarized conical split-beam patterns into half space. Its application is for the new radiodetermination satellite service (RDSS), just approved by the FCC.

During the past few years, several antennas such as microstrip patches [1] and spiral horns [2] have been introduced for mobile communications. Both types of antennas have used hybrid circuits to produce two split broad conical beams. The ideal RF performance is to maximize the peak gain (>5 dBi) while maintaining a broad halfpower beamwidth ($>40^\circ$). The antenna presented here has radiation fields that can be controlled by adjusting aperture radius and modes of excitation (TE_{21} or TE_{31}). Radiation patterns are calculated by aperture integration. Measured radiation patterns show that good symmetry exists and that the maximum beam axis occur at plus and minus 40° . Halfpower beamwidths of approximately 40° have been achieved.

THEORETICAL BACKGROUND

The basic electromagnetic principle applied to the analysis of this antenna is Huygen's secondary source to solve integral equations for vector potentials. Radiation patterns are calculated by aperture integration over a cylindrical cavity excited by higher order modes. The radiation fields in spherical coordinates for linear polarization (E_1 & E_2) can be obtained from Silver [3]. These fields can be circularly polarized by introducing a 90° phase difference. Physically, this corresponds to phasing adjacent probes with a 90° phase difference as shown in Figure 1.

For circular polarization and desired mode excitation, probes with proper spacing are needed. These probes are located perpendicular to the side wall so that their positions are parallel with the maximum E-field vector. The fields generated from two adjacent probes are orthogonal to each other inside the circular waveguide. With this angular spacing (α) chosen, as shown in Figure 1, one probe is always situated in the null field region of the other probe, thus causing very little mutual coupling between probes [1]. In order to keep beam symmetry (Omni-Directional in azimuth) and cross polarization low, many probes should be used to suppress unwanted modes. To determine the radiation pattern for circular polarization the following equation is used:

$$E_{TE_m} = \sum_{n=1}^N E_1 \sin(m\Phi) e^{j(n-1)\pi/2} \\ \pm j \sum_{n=1}^N E_2 \cos(m\Phi) e^{j(n-1)\pi/2}$$

WHERE:

N = number of probes
 α = $360/N$ degrees
 m = $N/4$ (mode number)
 Φ = $(\phi + (n-1)\alpha)$

RADIATION PATTERN AND GAIN CALCULATION

Radiation patterns are calculated by the equation depending on the mode excitation. Gain calculation is on the basis of $G=4\pi P_k/P_t$, where P_k is the peak power at the beam peak axis and P_t is the total power radiated. Radiation patterns are shown in Figure 2 for different modes. Gain computations are also illustrated in Table 1 for both different modes and diameters.

On the basis of Table 1 and Figure 2, radiation patterns and gains are in very close relationship to each other. Usually as aperture diameter increases, higher order modes are used. Since gains of modes 2 and 3 are approximately above 5dB and beam axis is controlled between 30° and 50°, radiation pattern and gain can be optimized, depending on requirements.

TABLE 1 CALCULATED GAIN AND RADIATION PATTERN

MODE (TE)	DIAMETER (WAVELENGTH)	PEAK DIRECTION FROM BROADSIDE	GAIN (dBi)	*BEAMWIDTH
1	.6	0°	8.3	90°
	.8	0°	10.9	74°
	1.0	0°	11.8	60°
2	1.0	41°	5.73	54°
	1.1	38°	6.75	50°
	1.2	36°	7.52	46°
3	1.34	51°	3.66	49°
	1.4	50°	5.32	48°
	1.46	48°	6.0	47°
4	1.7	56°	3.25	46°
	1.8	54°	5.13	44°
	1.9	52°	5.99	42°

***BEAMWIDTH IS ONE SIDE FOR TE₂₁, TE₃₁, AND TE₄₁**

EXPERIMENTAL RESULTS

Two prototype antennas (TE₂₁, 8 probes and TE₃₁, 8 probes) were fabricated to verify their predicted performances. Each prototype consisted of a circular waveguide cavity, feed probes and off-the-shelf power dividers. In order to provide the proper phase difference between probes, coaxial delay lines were connected between the probes and power dividers.

Comparisons between calculated and measured data are shown in Figure 3 and 4. Radiation patterns with TE₂₁ and TE₃₁ have shown that a good symmetric, conical pattern exists and that both beam axis and beam widths satisfy calculated results.

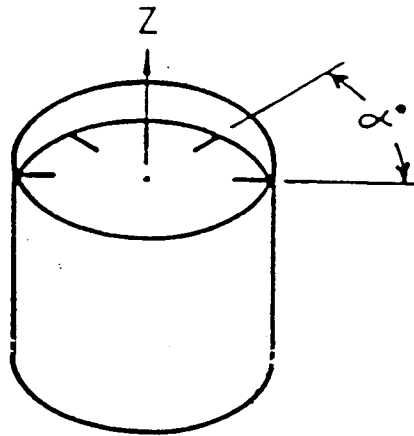


FIGURE 1

CIRCULAR WAVEGUIDE CAVITY SHOWING PROBES WITH ANGULAR SPACING α .

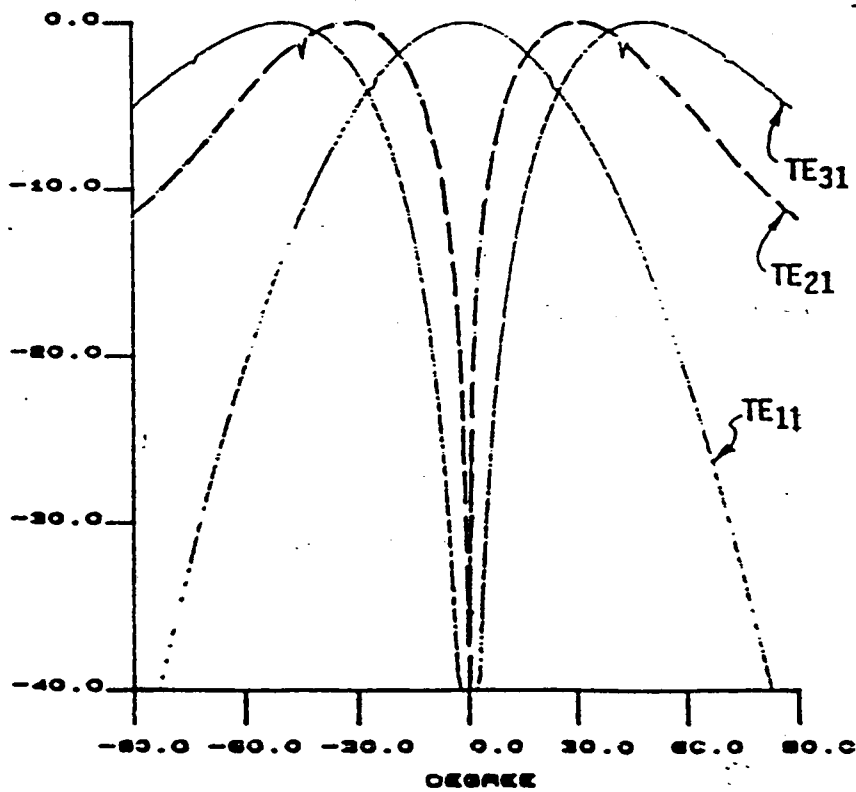


FIGURE 2

CALCULATED RADIATION PATTERNS FOR DIFFERENT MODE EXCITATIONS.

ORIGINAL PAGE IS
OF POOR QUALITY

FIGURE 3

COMPARISON BETWEEN COMPUTED AND
MEASURED PATTERNS, TE_{21} , DIA.
10.2"
 $F = 1.27$ GHz

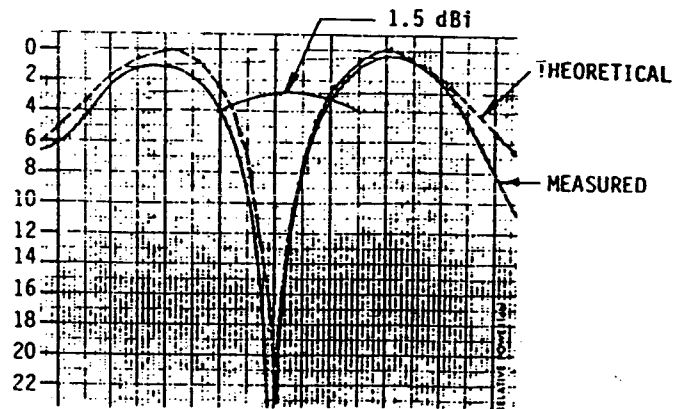


FIGURE 4

COMPARISON BETWEEN COMPUTED AND
MEASURED PATTERNS, TE_{31} , DIA.
11.5"
 $F = 1.62$ GHz

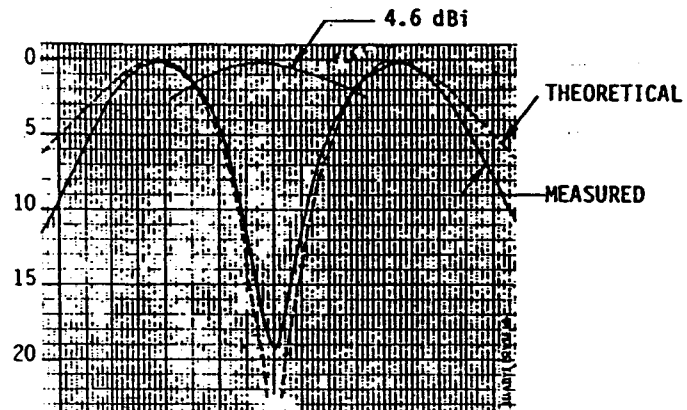
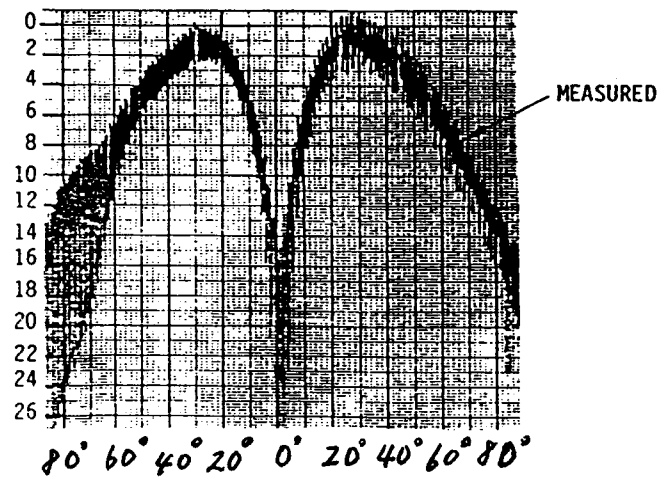


FIGURE 5

AXIAL RATIO PATTERN, TE_{21} , DIA.
10.2"
 $F = 1.62$ GHz



The axial ratio in Figure 5 is within 2 - 3 dB near the main beam axis. The phase feeding circuitry is very sensitive to the antenna performance; small errors in phase-amplitude of the combiner and phase lines cause major changes in radiation patterns. Since edge diffraction terms are not included, errors exist between computed and measured data around 90° . Overall measured radiation patterns are in agreement with calculated values.

REFERENCES

1. J. Huang, "Circularly Polarized Conical Patterns from Circular Microstrip Antennas". IEEE Trans. on Antennas and Propagat., Vol. AP-32, No. 9, Sept. 1984, pp. 991-994.
2. R. Johnson and H. Jasik, "Antenna Engineering Handbook", McGraw-Hill Book Co., 1984 Edition. pp. 14.3 - 14.24.
3. Silver, "Microwave Antenna Theory and Design", New York, Dover 1965, pp. 334-341.